A HIGH–EFFICIENCY MILLIMETER–WAVE HOLOGRAPHIC POWER SPLITTER/COMBINER

M. Shahabadi, K. Schünemann, and H.–G. Unger*
Arbeitsbereich Hochfrequenztechnik
Technische Universität Hamburg–Harburg
D–21071 Hamburg, Germany
*Institut für Hochfrequenztechnik
Technische Universität Braunschweig
D–38023 Braunschweig, Germany

Abstract

A millimeter–wave power splitter/combiner working on the principles of holography is presented. A hologram which stores the holographic image of a number of beams has the function of a power splitting element. An input beam to this hologram causes the recorded beams to be reconstructed, which is none but a high–efficiency process of beam splitting. A measured efficiency of 93%, high isolation, and a relatively large bandwidth are demonstrated.

Introduction

DOUBTLESS power combining is of paramount importance for low–power solid–state sources of millimeter waves. The existing methods of power combining are assigned to two categories: *resonant* and *non–resonant* approaches [1]. In resonant methods, the sources coherently inject their energies into an eigenmode of a shielded [2] or an open resonator [3]–[5] while non–resonant methods are mainly based on spatial combining of the energy radiated by an array of mutually–locked oscillators [6]–[8]. To avoid mode competition in the former and grating lobes in the latter, the single sources should be arranged within a spacing dictated by the wavelength. At millimeter–wave frequencies, this requires therefore a geometrically small inter–element spacing, or rather circuit miniaturization. However, regarding the fact that the solid–state millimeter–wave sources usually possess a low power efficiency, these sources should be equipped with heat sinks which are as large as several wavelengths and represent an obstacle to circuit miniaturization.

To overcome these shortcomings and to allow sufficient spacing between the output (input) ports, we have recently introduced a novel approach to power splitting (combining) by means of holography [9]. In this method, power splitting is performed by a *computer–generated* hologram storing holographic images of a given number of electromagnetic beams. Illumination of this hologram with an appropriate input beam reconstructs the stored images coherently. In other words, the introduced holographic method offers an elegant way for splitting a beam into a set of coherent beams and vice versa. Furthermore, since the recorded beams can arbitrarily be oriented in the hologram, the spacing between them may be chosen large enough to avoid the aforementioned problem of miniaturization.

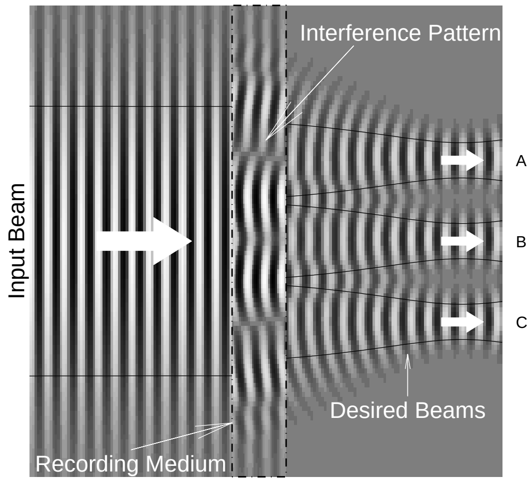

Fig. 1: Simulated interference pattern of an input beam with three output beams

Reporting on the implementation of a millimeter–wave holographic power splitter/combiner is the aim of this contribution, where we demonstrate a high beam splitting efficiency along with other appreciable characteristics like high isolation and bandwidth. Prior to a discussion about the realized power splitter/combiner, we concisely review the main aspects of holography and holographic power splitting.

Holographic Beam Splitting

Generally speaking, a hologram modulates the amplitude and/or phase of an incident wavefront [10]. A phase hologram[1] can be imagined as a recording medium with the capability to store the relative phase between two interfering wavefronts. When illuminated with one of these waves, the hologram restores the phase, and consequently the wavefront, of the second wave from the recorded phase difference. During this process, some usually low–power diffracted waves of higher order will also be generated.

According to this observation and for the purpose of beam splitting, one may choose the input beam and the beams to be produced as the interfering waves for

[1] We do not consider amplitude or absorption holograms since their inherent loss excludes them from being a candidate for a power combining/splitting element.

0-7803-4603-6/97/$5.00 (c) IEEE

a hologram so that exposing the hologram to the input beam produces the desired output beams. As long as the input and output beams are known analytically or experimentally, their interference pattern can numerically be simulated. For instance, Fig. 1 shows a simulated interference pattern of an input beam with three Gaussian output beams in the region labeled with *recording medium*. In the terminology of Fourier optics, the simulated interference pattern can be related to an *optical transfer function* for the recording medium or hologram. Evidently, we are interested in transfer functions which mainly modulate the phase distribution of the incident wave. In this case, the hologram is realized with, for example, a dielectric phase plate showing the required phase characteristic, and is therefore called a *computer–generated* phase hologram.

Not to mention that in the above computational procedure, the intensity of the input beam is assumed to be equal to the sum of the intensities in the output beams so that a high splitting efficiency will be maintained. In addition, one should pay attention to keeping the power level of the undesired diffracting orders as low as possible.

It is worth noting that in optics, a comparable holographic method has previously been proposed for multiple imaging [11]–[12] and beam addition [13]. The basic element in this method is an optical grating known as Dammann grating which diffracts an incoming plane wave, and produces a number of equi–power diffraction orders, i.e. discrete plane waves propagating in some defined directions. Thus a Dammann grating is based on Fraunhofer diffraction and works only in the far–field zone. However, due to the fact that the period of a Dammann grating amounts to several wavelengths, at typical millimeter–wave frequencies the far–field region of this grating exceeds several meters, so the method of references [11]–[13] is not practicable for millimeter waves. As opposed to this, the method introduced here is based on Fresnel diffraction and works in the near–field zone.

The coming section deals with the implementation of a prototype for holographic power splitting/combining.

Implementation

The introduced holographic approach has been implemented at 24 GHz in parallel–plate waveguide technique according to the arrangement of Fig. 2. It consists of *A)* a hologram, *B)* a horn array for collecting the output beams, and *C)* a setup to generate a readout beam for reconstructing the images recorded in the hologram.

A) Hologram

The heart of the configuration is a dielectric phase plate working as a hologram. To generate identical equidistant output beams that can effectively be collected by the horn array, the hologram should obviously store a periodic repetition of the holographic image of a single beam. Hence, the hologram is assumed to be a periodic structure the period of which equals that of the horn array. The phase characteristic of the hologram

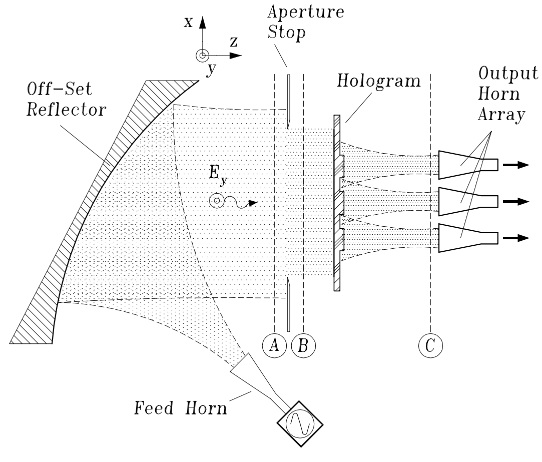

Fig. 2: A holographic power splitter

is obtained from the properties of both the input beam and the beams to be coupled to the output horn array. Knowing the needed phase characteristic for the hologram, we design the shape of a dielectric periodic structure in an iterative trial–and–error procedure to meet the required characteristic. During this procedure, the periodic structure is modelled by a transmission–line network proposed in [14], which facilitates the design process considerably.

B) Horn Array

The output horn array is composed of a number of H–plane sectoral horns. To investigate the field received by the array, it is considered as a conducting periodic structure. The field inside each horn is expanded in terms of the Hankel functions of the first and second kind. This expansion is matched, on the one hand, to the spatial harmonics in the aperture of the array, and on the other hand, to the eigenmodes of the feeding waveguide. Including the edge conditions completes the description of the horn array.

By using the above approach, a hologram storing the image of a horn array has been designed. The setup of Fig. 3 has been used to characterize the combination of the hologram and the horn array with the scattering parameters. The reflection, $|S_{11}|$, and mutual coupling, $|S_{21}|$, measured with a *HP 8510C* network analyzer, are seen in Fig. 4 and 5, respectively. The results not only verify our computation (dot–dash curves) but also indicate a return loss of better than 15 dB and an iso-

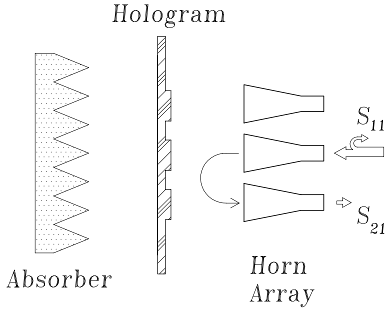

Fig. 3: Setup to measure the scattering parameters

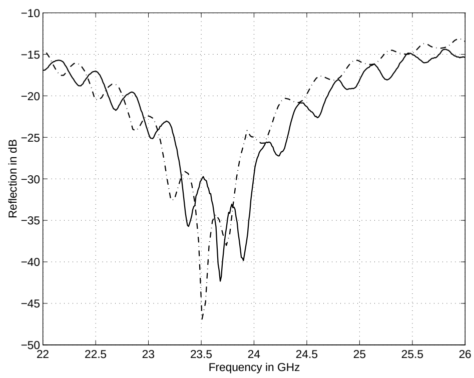

Fig. 4: Measured '−' and computed '−·' reflection

lation of higher than 25 dB over a bandwidth of more than 15%. The slight deviation of the measured values from the simulated ones is probably caused by the ohmic losses on the walls of the horn antennas.

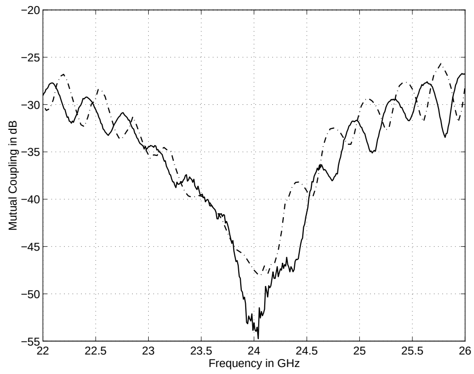

Fig. 5: Measured '−' and computed '−·' mutual coupling

C) Readout Beam

To generate a beam for reading the stored images in the hologram, the setup of Fig. 2 involves a feed horn, an off–set reflector, and an aperture stop. The off–set reflector having a diameter of $48\lambda_0$ is illuminated by the feed horn and provides a nearly Gaussian beam as shown in Fig. 6. This figure illustrates the measured field intensity along line **A** of Fig. 2 in the absence of other components of the setup. The field intensity evaluated by using the moment method is also shown in the same figure. For an equi–power reconstruction of the recorded images, the hologram should be excited with a uniform (flat–top) beam. In Fig. 2, the $18\lambda_0$–wide aperture stop passes a portion of the Gaussian beam, and flattens the field profile. The normalized field intensity measured across line **B** (Fig. 2) as well as the moment–method simulation of the stop are seen in Fig. 7. It should be noted that the applied procedure of beam equalizing is not an efficient one and shows an efficiency of only 70%[2]. For a more efficient beam equalization, one can use lens–like refractive components [15], improve the feed system of the reflector, or modify the shape of the reflector [16].

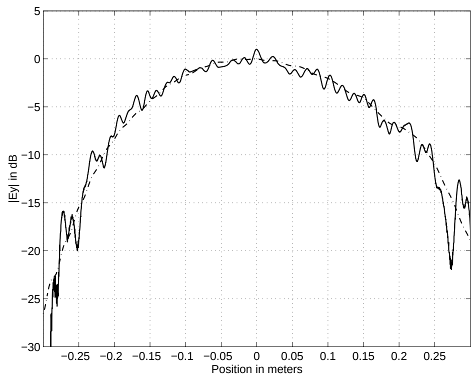

Fig. 6: Nearly Gaussian beam reflected from the reflector (measured '−', computed '−·')

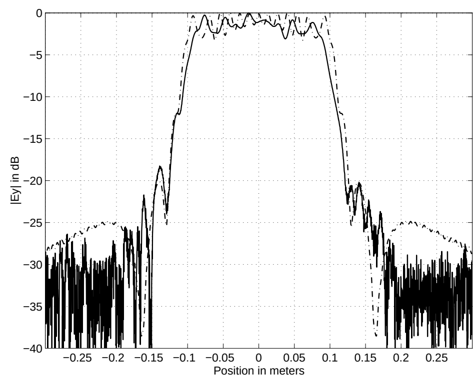

Fig. 7: Equalized beam by the aperture stop (measured '−', computed '−·')

Fig. 8 depicts the measured field intensity across line **C** of Fig. 2. It can clearly be seen that the hologram has reconstructed the three recorded beams. The theoretical field distribution shown in Fig. 8 has been computed with the help of the method developed in [14]. Note the excellent agreement between the measured and computed values. See Fig. 9 for the simulated electric field distribution in response to a Gaussian input beam. Three reconstructed beams and some higher diffraction orders are readily recognized in this figure.

The transmission characteristic between the feed horn and each output horn has been measured using a *HP 8510C* network analyzer. The result seen in Fig. 10 shows an overall transmission of -8 ± 0.5 dB for all outputs. Owing to the limited efficiency of the beam–equalizing stop and regarding the ohmic losses in the parallel–plate waveguide, the measured power of the beam incident on the hologram is about 50% of the total input power, so an overall transmission of -8 ± 0.5 dB indicates that 93% of the power incident on the hologram has been received by the output horns. In the case that the hologram is absent, the power received by the array diminishes to only 25%.

The ripples observed in the frequency response are

[2]The efficiency is defined as the ratio of the power leaving the stop to the power incident on it. Since both incident and transmitted beam are paraxial, the efficiency η has been estimated by

$$\eta \approx \frac{\int |E_y(B)|^2 dx}{\int |E_y(A)|^2 dx},$$

where $|E_y(A)|$ and $|E_y(B)|$ are the measured amplitudes of the field along lines A and B of Fig. 2, respectively.

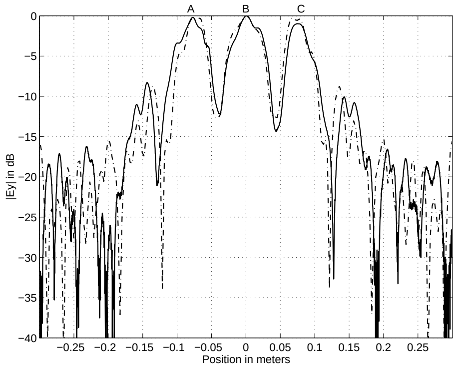

Fig. 8: Reconstruction of the stored beams (measured '–', computed '–·')

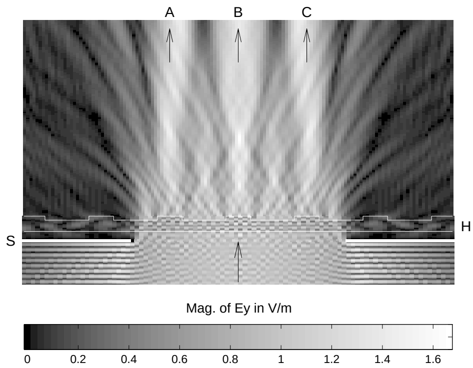

Fig. 9: Electric field distribution (H: Hologram, S: Stop, and A,B,C: Output beams)

caused by multiple reflections between the reflector and the aperture stop, and will vanish by replacing the stop with a matched refractive beam equalizer. With the stop, the isolation between the output ports is better than 17 dB over the frequency band shown in Fig. 10. It should be added that, in this prototype, the spacing between the output ports is larger than $6\lambda_0$, and can be made even higher, which demonstrates the scalability of this method up to very high frequencies.

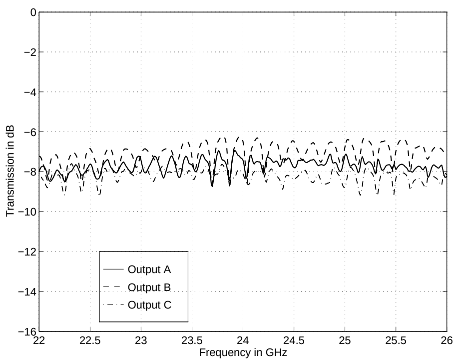

Fig. 10: Overall transmission factor for each output

Conclusions

A holographic power splitter/combiner has been presented. It is capable of becoming a favorite candidate for millimeter–wave applications because of its high efficiency, broadband character, high isolation, and flexibility in the orientation and the number of outputs.

Acknowledgment

The authors wish to thank the Deutsche Forschugsgemeinschaft for financial support of this project.

References

[1] K. Chang, C. Sun, "Millimeter–Wave Power–Combining Techniques," *IEEE Trans. Microwave Theory Tech.*, vol. MTT–31, pp. 91–107, Feb. 1983.

[2] K. Chang, W. F. Thrower, and G. M. Hayashibara, "Millimeter–Wave Silicon IMPATT Sources and Combiners for the 110–260-GHz Range," *IEEE Trans. Microwave Theory Tech.*, vol. MTT–29, pp. 1278–1284, Dec. 1981.

[3] L. Wandinger, V. Nalbandian, "Millimeter–Wave Power Combiner Using Quasi–Optical Techniques," *IEEE Trans. Microwave Theory Tech.*, vol. MTT–31, pp. 189–193, Feb. 1983.

[4] J. W. Mink, "Quasi–Optical Power Combining of Solid–State Millimeter–Wave Sources," *IEEE Trans. Microwave Theory Tech.*, vol. MTT–34, pp. 273–279, Feb. 1986.

[5] J. Bae, Y. Aurakawa, H. Kondo, T. Tanaka, and K. Mizuno, "Millimeter and Submillimeter Wave Quasi–Optical Oscillator with Gunn Diodes," *IEEE Trans. Microwave Theory Tech.*, vol. MTT–41, pp. 1851–1855, Oct. 1993.

[6] K. D. Stephan, "Inter–Injection–Locked Oscillators for Power Combining and Phased Arrays," *IEEE Trans. Microwave Theory Tech.*, vol. MTT–34, pp. 1017–1025, Oct. 1986.

[7] Z. B. Popovic, D. B. Rutledge, "Diode–Grid Oscillators," *IEEE Antennas and Propagation Symposium*, pp. 442–445, Syracuse 1988.

[8] R. A. York, R. C. Compton, "Quasi–Optical Power Combining Using Mutually Synchronized Oscillator Arrays," *IEEE Trans. Microwave Theory Tech.*, vol. MTT–39, pp. 1000–1009, June 1991.

[9] M. Shahabadi, K. Schünemann, "Holographic Power Combining: A New Principle for Millimeter and Submillimeter–Wave Power Combining," *The 26th European Microwave Conference*, pp. 115–119, Prague, Czech Republic, Sept. 1996.

[10] H. M. Smith, "Principles of Holography", *John Wiley & Sons*, 2nd Edition, 1975.

[11] S. Lu, "Generating Multiple Images for Integrated Circuits by Fourier–Transform Holograms," *Proc. IEEE*, vol. 56, pp. 116–117, Jan. 1968.

[12] H. Dammann, K. Görtler, "High–Efficiency In–Line Multiple Imaging by Means of Multiple Phase Hologram," *Optics Communications*, vol. 3, pp. 312–315, July 1971.

[13] J. R. Leger, G. J. Swanson, and W. B. Veldkamp, "Coherent Beam Addition of GaAlAs Lasers by Binary Phase Gratings," *Appl. Phys. Lett.*, vol. 48, pp. 888–890, April 1986.

[14] M. Shahabadi, K. Schünemann, and H.–G. Unger, " Modelling of Diffraction at Dielectric Biperiodic Objects Using an Equivalent Network," *The 20th International Conference on Infrared and Millimeter Waves*, pp. 397–398, Orlando, USA, Dec. 1995.

[15] J. L. Kreuzer, "Coherent Light Optical System Yielding an Output Beam of Desired Intensity Distribution at a Desired Equiphase Surface," US Patent 3 476 463, Nov. 1969.

[16] D.–W. Duan, Y. Rahmat–Samii, "A Generalized Diffraction Synthesis Technique for High Performance Reflector Antennas," *IEEE Trans. Antennas and Propagation*, vol. AP–43, pp. 27–40, Jan. 1995.

0-7803-4603-6/97/$5.00 (c) IEEE